Onboard measurements of pressure pulsations in a low specific speed Francis model runner

IOP Conf. Series: Earth and Environmental Science **240** (2019) 022040 doi:10.1088/1755-1315/240/2/022040

Onboard measurements of pressure pulsations in a low specific speed Francis model runner

E Agnalt, B W Solemslie, O G Dahlhaug

Waterpower Laboratory, Department of Energy and Process Engineering, NTNU - Norwegian University of Science and Technology, Trondheim, Norway

E-mail: einar.agnalt@ntnu.no

Abstract. Over the last years, there have been several incidents with cracks in high head Francis turbines. These cracks are understood to be related to pressure pulsations, vibration modulus and the combination of these. In this paper, a setup for the investigation of pressure pulsations in a low specific speed model turbine is presented with the use of onboard pressure sensors. Earlier onboard measurements have mainly utilized blade-mounted sensors. In this paper, a setup with hub-mounted pressure sensors are described. In addition, a position sensor is utilized to analyse the pressure data relative to the angular position of the runner. The setup is considered as a good reference for computational fluid dynamics validation and is considered less extensive for evaluating the onboard pressure pulsations compared to blade-mounted sensors.

1. Introduction

Some new power plants with installed Francis turbines have experienced breakdown after few hours of operation. The design and calculations of Francis runners are based on numerical analysis, but the main problem is the validation of the results regarding fluid structure interaction in the runner. For a better understanding of the physics behind this problem, measurements must be performed for the validation of the numerical results.

Measurements including moving fluids and transient properties, as pressure pulsations, could be severely influenced by the mounting method of the sensor [1,2]. Today, pressure sensors with high accuracy and small sizes are available with flush mounted diaphragm. For application where accurate flush mounting is possible, the uncertainty from mounting related to hole size, transmission tubes and cavities will be removed[3]. The time and frequency response for the measurements is only related to dynamic properties of the diaphragm and the acquisition chain as described in the ISA standard "A Guide for the Dynamic Calibration of Pressure sensors"[4]. In the current measurements, flush mounting of the sensors was selected to reduce uncertainty related to the mounting method.

To analyze the pressure in the runner channel, the main method found for onboard pressure measurements, are with the use of miniature blade-mounted sensors. Several studies utilized onboard measurements with blade mounted miniature sensors [5–11]. Kobro et.al did onboard measurements on the same runner as described in this paper, but the complexity of the setup and durability of the sensors was not satisfactory[12]. Another concern is the possibility for mechanical influence on the pressure sensors if mounted on thin blades. The setup presented utilizes a measurement method with hub mounted pressure sensors to analyze the pressure pulsations onboard a low specific speed Francis model runner.

The data acquisition in the rotating domain can be done with different methods including telemetry, slip-ring, onboard acquisition and a combination of onboard acquisition and digital transfer with a slip-ring. In the presented setup, a parallel sampling data acquisition system for all measurements were selected to avoid uncertainties related to time synchronization, hence a multi-channel analog slip-ring system was used.

In addition to the onboard pressure measurements, a setup for continuous angular position measurement of the runner is presented. The objective of the measurements is the analysis of onboard pressure relative to runner angular position.

2. Methods

2.1. Experimental setup

The Francis test-rig available at the Waterpower laboratory, at Norwegian University of Science and Technology was used for the experimental studies[13,14]. The Francis turbine in the test-rig is shown in Figure 1.

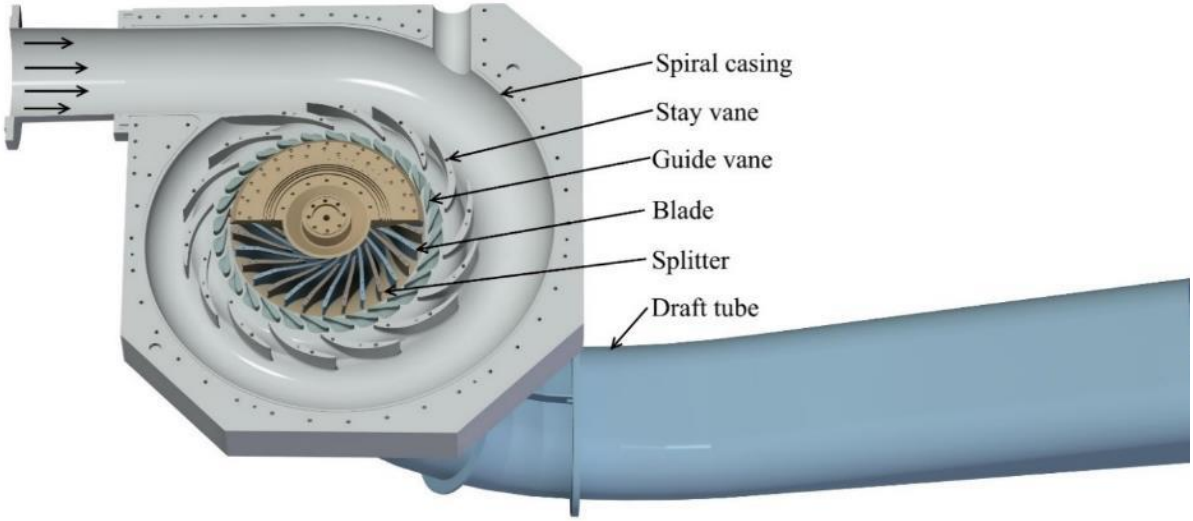

Figure 1 Three-dimensional view of the investigated Francis turbine.

The Francis turbine was equipped with all required instruments to conduct model testing according to IEC 60193[15]. The total number of pressure taps in the experimental setup was 24. In this paper, the focus was on four sensors mounted in the runner. Figure 2 shows the locations of the onboard pressure sensors in the turbine (R1, R2, R3 and R4). The onboard sensors were mounted in the runner crown. Due to space restriction and the number of channels in the slip ring, custom amplifiers were built and mounted onboard the runner.

To analyze the pressure values onboard the runner relative to the stationary frame, a position sensor (Z) was added to the shaft. The sensor was a digital encoder with 13 bit resolution. The digital position signal was converted to analog +/-10V saw tooth to reduce the number of leads in the cable, and for easier synchronization of other analog values in the DAQ system. The position sensor is shown in Figure 3

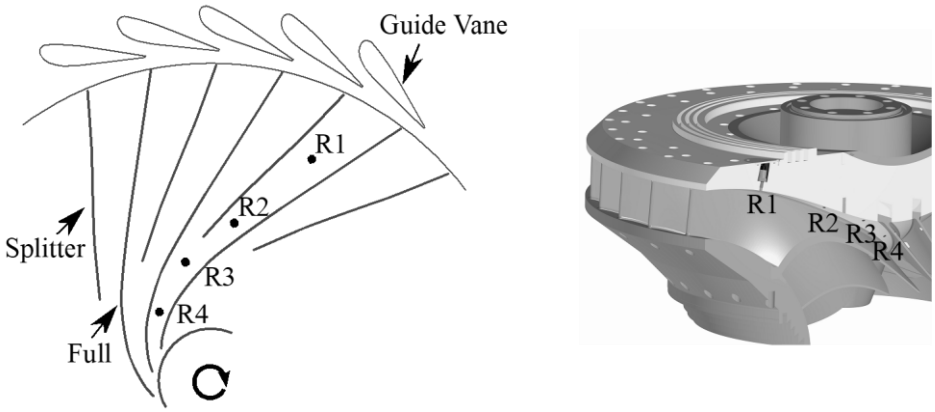

Figure 2. Onboard pressure sensors R1 to R4.

Figure 3. Position sensor Z. A digital absolute encoder measures the angular position with binary output. The binary signal is converted to analog value with a digital to analog converter (DAC).

2.2. Data acquisition

The data acquisition system (DAQ) for the onboard measurements, was built with the use of slip-ring. This was chosen to enable full time-synchronisation between stationary and rotating domain, which was of great importance when relating the onboard measurement to runner position measured in the stationary domain. This approach does however introduce longer signal transfer with analog voltage and is therefore more susceptible to noise. This could be reduced with differential signal transfer, but with limited number of channels in the slip-ring, single ended data transfer were selected with common ground. A differential signal transfer, where each channel has signal and reference, would be more noise resistant. A comparison between a single ended and differential signal transfer confirmed this. Nevertheless, in the uncertainty analysis, the added noise did not affect the total uncertainty in the measurements. The input to the DAQ system had low-pass filters for anti-aliasing and the total number of channels in the measurement campaign were 50.

The onboard amplifiers were design with programmable gain instrumentation amplifiers and a precision voltage reference for excitation voltage to the sensors. The amplifiers were design with dual power supply to utilize the full range of the +/-10V input to the DAQ system. One amplifier and a connector board is shown in Figure 4. The amplifiers were mounted inside the runner, i.e as close as possible to the signal source, to improve noise resistance.

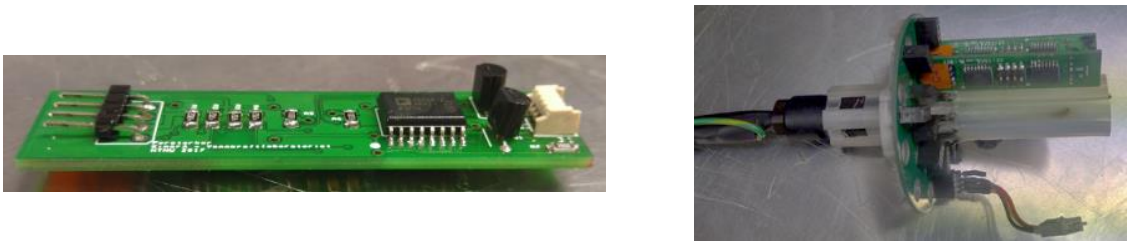

Figure 4. Onboard amplifiers, single card and two amplifiers mounted in a connector. The connector with the amplifiers were mounted inside the runner.

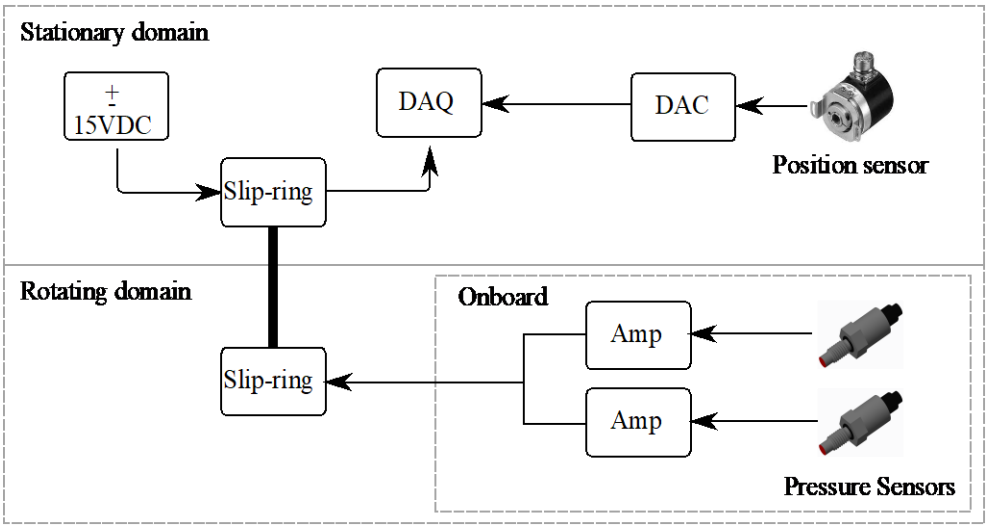

Figure 5. Data acquisition setup.

2.3. Measurements

The setup presented in this paper, was utilized for several measurements and operational conditions. The results for this paper are based on the measurement presented in Table 1.

Table 1. Measurement summary. Alpha is guide vane opening.

Description	N_{ED}	Q_{ED}	Head	Alpha	Speed
Best Efficiency Point (BEP)	0.180	0.154	15.6 m	10 °	382.7 rpm

2.4. Post processing methods

The position sensor was used to analyse the onboard measurements relative to stationary domain. The raw signal from the position sensor was +- 10V saw tooth signal representing one revolution of the runner as presented in Figure 6. The digital to analog conversion of the position from the encoder was operation in transparent mode, meaning all changes of position was continuously updated on the analog output. This gave glitches on the signal which needed to be filtered. A local regression smoothing filter was used. The signal was then converted to a continuous increasing position vector and the first derivative was calculated to find the speed vector.

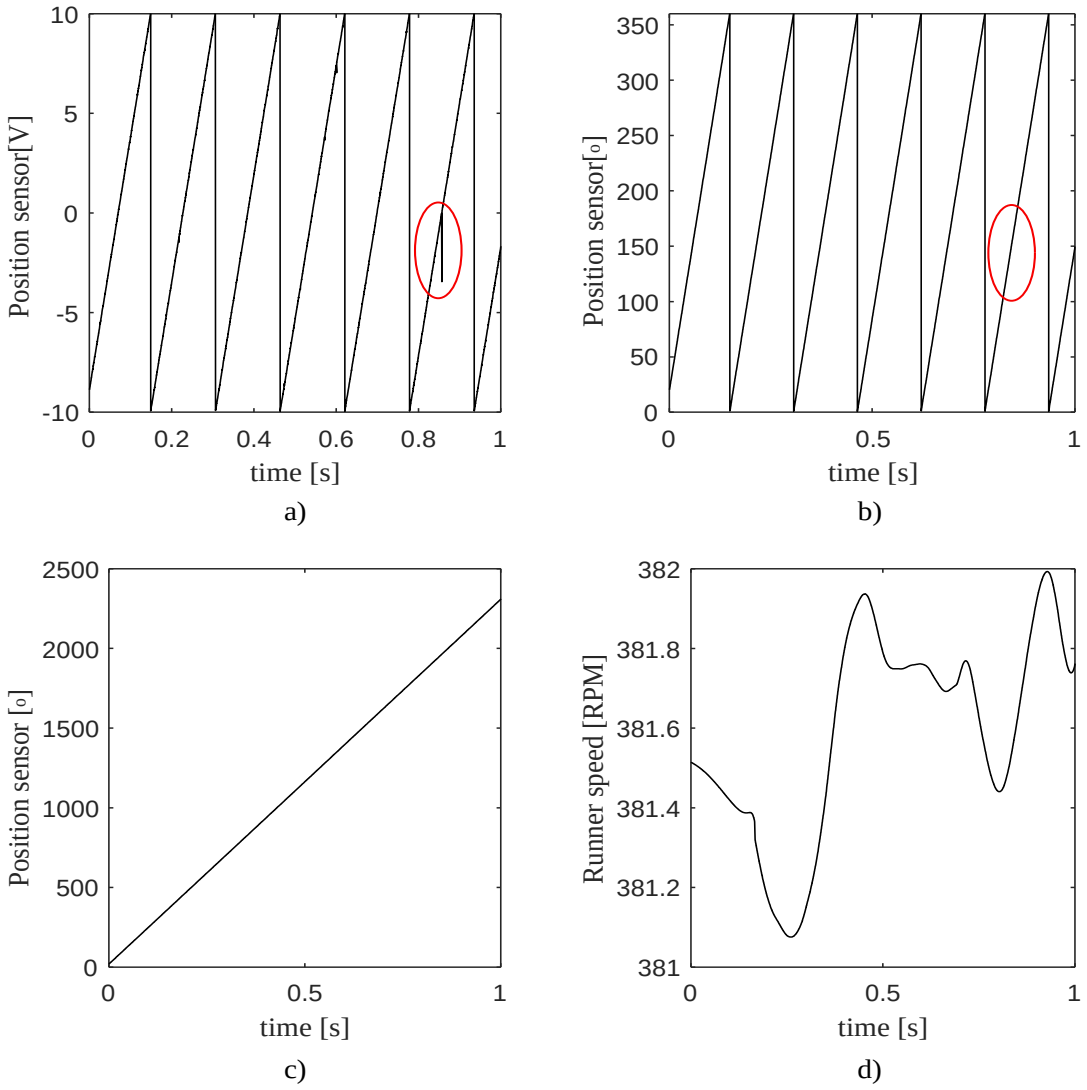

Figure 6. Position sensor signal processing. a) Saw tooth raw data from sensor. The signal includes some noise and glitches from the digital to analog conversion (circled). b) The signal is filtered using local regression smoothing. c) A continuous vector is created from the saw tooth signal by adding 360º for each drop. d) First derivative of the signal gives the speed vector.

2.5. Calibration and uncertainty

The pressure sensors was initially calibrated in the estimated pressure range for the measurements using the guidelines of German Calibration Service [16]. This guideline is according to the ISO guide to uncertainty of measurements[17]. To ensure accuracy, the whole measurement chain is taken into account in the calibration, in accordance with the recommendations in IEC 60193[15]. For practical reasons, the slip ring was not spinning during calibration, but a separate test was performed with a constant precision voltage source without any added uncertainty. The effect of runner rotation was tested in air by spinning the runner at rated speed, but the influence was found to be neglectable. The calibration constants for each sensor were found with linear regression and the deviation between the calibration reference and the sensor output was used for the estimation of uncertainty. To further evaluate the long-time stability and temperature sensitivity of the sensors, substitute calibration were conducted in zero flow conditions at start up and stop each measurement day. The substitute sensor was calibrated and mounted on the draft tube cone. Figure 7 shows the calibration results for pressure sensor R1 and the

limits of deviation including the long-time stability. A summary of the calibrated expanded uncertainties for all pressure sensors is found in Table 2 for BEP. The expanded uncertainties is calculated with a coverage factor of 2 which for a measurand with normal distribution represents a coverage probability of approximately 95%.

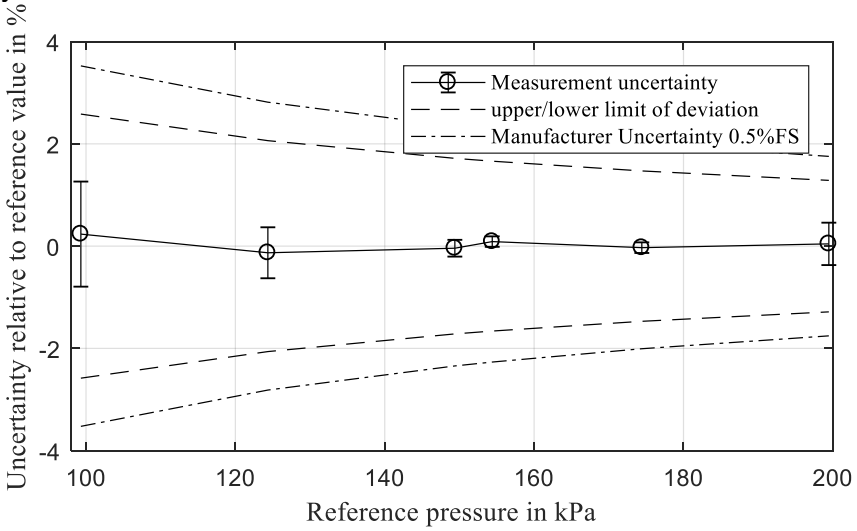

Figure 7. Calibration result for R1. Measurement uncertainty is uncertainty from initial calibration. Upper and lower limits includes the long-time repeatability of the sensor related to the reference sensor mounted in the draft tube cone. Manufacturer uncertainty is shown for reference.

For the evaluation of amplitudes, which is a dynamic property, the static calibration may not be valid[18]. If the frequency response function of the system is known, the dynamic uncertainty could be modelled[19]. In the current measurement setup, all sensors are stated to have resonance frequencies above 25kHz. Frequencies of interest are below 1,2% of resonance, hence it is assumed that the dynamic uncertainty is neglectable and only repeatability and hysteresis from static calibration remains in the uncertainty evaluation due to covariance[20]. In Figure 8, the 95% absolute repeatability in kPa for the calibrated points for sensor R1 are presented.

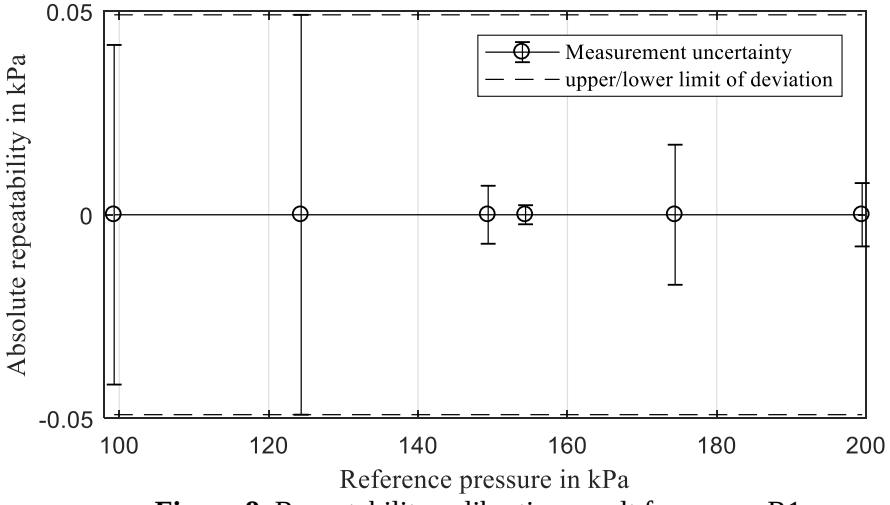

Figure 8. Repeatability calibration result for sensor R1.

To analyse the repeatability of the experiments and the test rig, BEP was recorded at the beginning and end of each day the measurements were performed. The 95% probability limits of the difference between reference and each sensor was calculated as presented in Table 2

Table 2. Uncertainty budget for mean pressure, BEP.

Location	Type / Full scale range	Mean pressure [kPa]	Expanded calibrated uncertainty [kPa]	Expanded long time stability [kPa]	Expanded measurement repeatability [kPa]	Total Expanded uncertainty [kPa]
R1	Entran/7bara	128	0.8	2.1	2.6	3.0 (2.3%)
R2	Entran/7bara	101	1.2	3.0	2.2	3.7 (3.7%)
R3	XP5/2bara	88	0.6	1.1	0.7	1.3 (1.5%)
R4	XP5/2bara	80	0.2	0.9	1.0	1.3 (1.6%)

Uncertainty budget for the amplitudes RSI amplitudes is presented in Table 3

Table 3. Uncertainty budget for RSI amplitudes, BEP.

Location	Type/Fs	Repeatability [kPa]	Amplitude RMS of fundamental frequency RSI [kPa]	Relative Uncertainty [%]	Amplitude RMS of first harmonic RSI [kPa]	Relative Uncertainty [%]
R1	Entran/7bara	0.05	1.17	4.3	0.08	63
R2	Entran/7bara	0.05	0.88	5.7	0.06	83
R3	XP5/2bara	0.02	0.67	3.0	0.04	50
R4	XP5/2bara	0.02	0.39	5.1	0.02	100

The uncertainty of the position measurement is related to linearity of the position sensor (0.05º), conversion rate of the digital analog converter (neglectable) and signal noise and the post-processing filtering (0.4º). The uncertainty related to signal noise and post-processing was found from the difference in raw signal and filtered signal. In addition, the anti-aliasing filter of all other sensors gave a time-delay which gave an added uncertainty as a function of rotational speed (0.2º at 380rpm). The total maximum absolute position uncertainty was 0.45º.

3. Results and discussion

The small speed variation in Figure 6d will in a fast Fourier transform give possible spectral leakage if not properly configured. To remove the effect of small changes in the rotational speed, the measured onboard signals were resampled to a fixed rate position signal. With small speed variation, rotational steps of the position vector was nonuniform. The nonuniform steps are represented by the speed vector in Figure 6d, since speed is first derivative of position. The resample process interpolates the measurands to a fixed number of equally spaced sample points per revolution. To verify the resampling process, FFTs of the signal were calculated before and after resampling. Figure 9a is for reference with ten flat-top windows overlapping with 50%. The results gives good amplitude prediction for both signals, but the frequency resolution is low. It is well know that longer windows in FFT will give higher frequency resolution, but varying frequencies will give spectral leakage and thereby reduce amplitude accuracy[20]. This is shown in Figure 9b, were a single window is used for a 30 second measurement. As seen in the figure, the resampled signal is unaffected by the leakage and maintains the correct amplitude. The conversion to positional domain is therefore considered particularly useful if evaluating speed dependent frequencies in variable speed measurements with short time FFT.

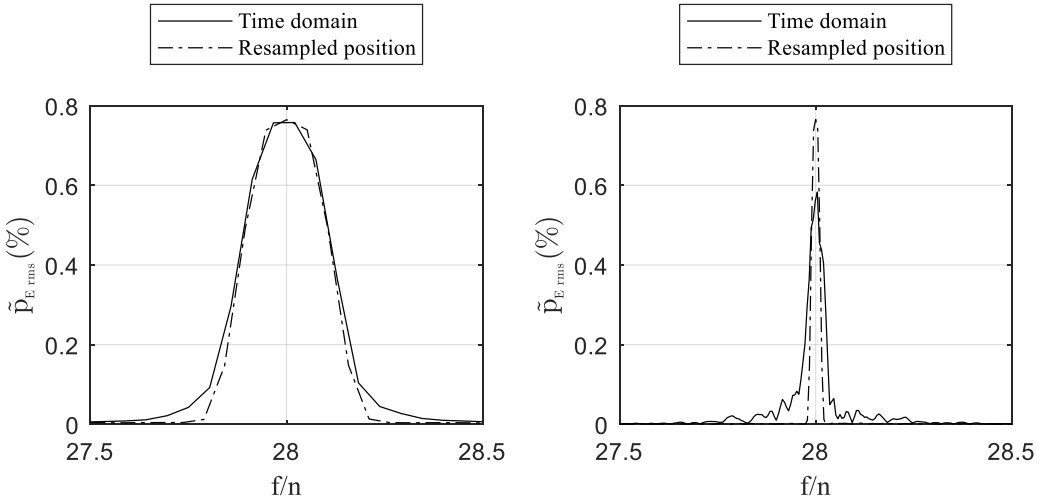

a) b)

Figure 9. FFT comparison of time domain data and resampled position domain data for guide vane passing fundamental frequency. a) Reference calculation to show unaltered amplitude prediction b) Longer windows for higher frequency resolution, unaffected amplitude accuracy for resampled signal.

Figure 10 shows the measured pressure for R1-R4 for one revolution of the runner. A moving average was calculated for each sensor with window length equal to ten revolution of the runner to avoid filtering of the frequency content of the signal. An uncertainty band was added according to the uncertainties presented in Table 2.

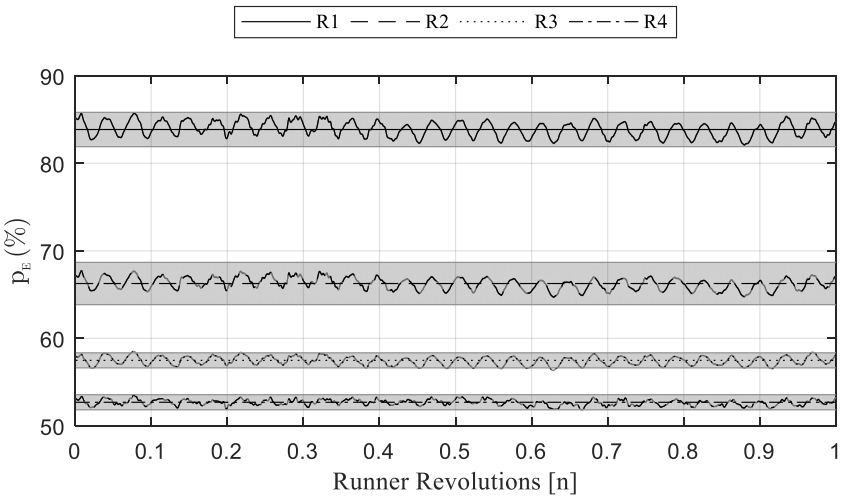

Figure 10. Measured pressure in position R1 to R4. A moving average is calculated for each sensor. The shaded area represents the uncertainty of the moving mean.

To analyse the frequencies in the signals, Fast Fourier Transform (FFT) with Welch method was used. The frequency with predominant amplitude is the guide vane passing frequency as shown in Figure 11.

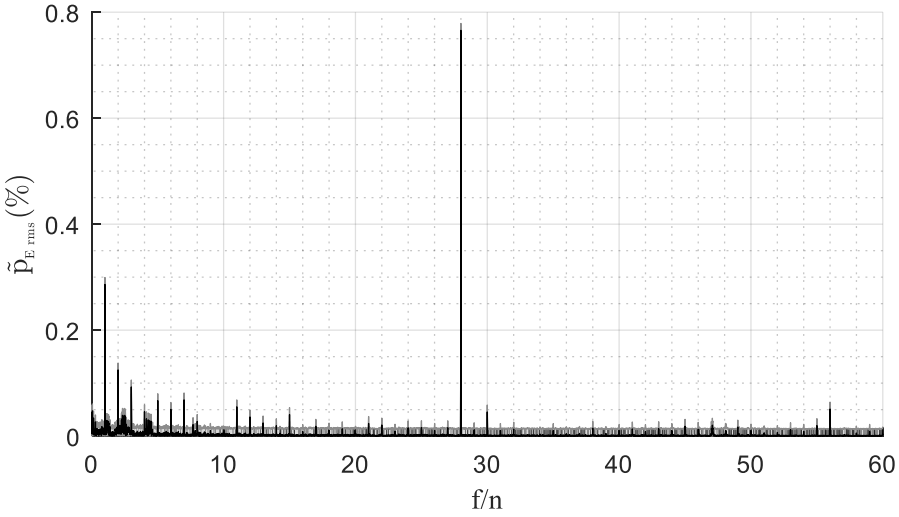

Figure 11. FFT R1 in time domain normalized to runner frequency. Grey shaded area represents uncertainty according to **Table 3**.

By dividing the angular position into 360 sectors, the pressure for each rotational degree of the runner was analysed. In Figure 12, the mean pressure in each sector for 191 revolutions is presented for sensor R1. The standard deviation for each sector was also calculated and indicated as a 95% interval. This analysis provides information of the pressure for both random and systematic quantities.

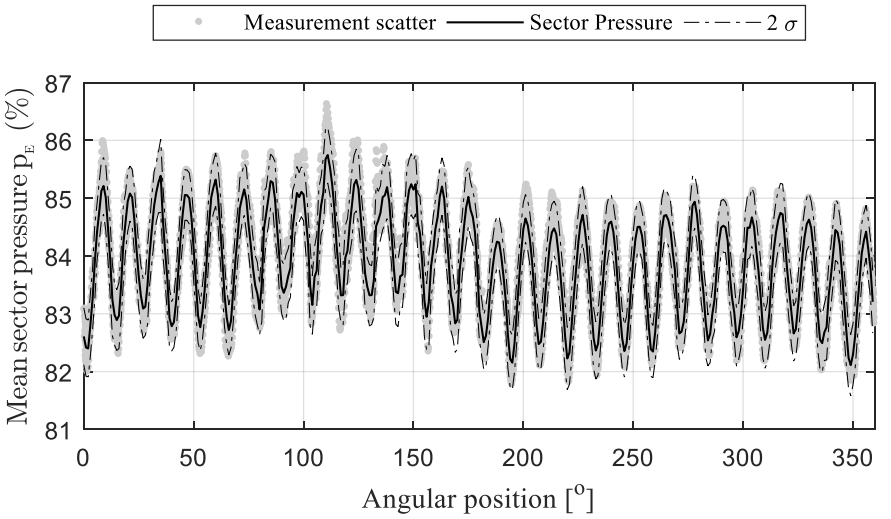

Figure 12. Mean pressure of R1 in one degree angular sectors, calculated from 191 revolutions of the runner.

4. Conclusion

The measurement setup is considered to give valuable data for CFD verification and the study of onboard pressure in the runner. Combined with a CFD analysis, this could provide valuable information for explaining the physics in the runner channel. The position resampled signal is considered to increase the accuracy of measurement analysis. For the mean pressure, the uncertainty of the measurements was mostly affected by the zero stability of the sensors and the repeatability of the measurements. The evaluation of fluctuating quantities is less affected by the uncertainties in the mean pressure. The RSI frequency is found to be the frequency with predominant amplitude in the channel.

References

[1] Rayle R E 1949 *An investigation of the influence of orifice geometry on static pressure measurements* Thesis (Massachusetts Institute of Technology)
[2] H.Bergh and H.Tijdeman 1965 *Theoretical and experimental results for the dynamic response of pressure measuring systems* (Nationaal Lucht- En Ruimtevaartlaboratorium Report)
[3] Franklin R e. and Wallace J M 1970 Absolute measurements of static-hole error using flush transducers *J. Fluid Mech.* **42** 33–48
[4] ISA 2002 *A guide for the dynamic calibration of pressure transducers* (67 Alexander Drive, P. O. Box 12277, Research Triangle Park, North Carolina 27709: ISA)
[5] Farhat M, Natal S, Avellan F, Paquet F, Lowys P Y and Couston M 2002 Onboard Measurements of Pressure and Strain Fluctuations in a Model of low Head Francis Turbine. Part 1 : Instrumentation *Proc. 21st IAHR Symp. Hydraul. Mach. Syst.* 865–72
[6] Perrig A, Avellan F, Kueny J-L, Farhat M and Parkinson E 2005 Flow in a Pelton Turbine Bucket: Numerical and Experimental Investigations *J. Fluids Eng.* **128** 350–8
[7] Pierre-Yves Lowys, Jean-Loup Deniau, Eric Gaudin, Pierre Leroy and Mohand Djatout 2006 On-board model runner dynamic measurements HydroVision (Portland: HCI Publications)
[8] Jansson I and Cervantes M 2007 A method to flush mount replaceable pressure sensors on a 9.3 MW prototype of a Kaplan runner *Proceedings of the 2nd IAHR International Meeting of the Workgroup on Cavitation and Dynamic Problems in Hydraulic Machinery and Systems,* IAHR International Meeting of the Workgroup on Cavitation and Dynamic Problems in Hydraulic Machinery and Systems : 24/10/2007 - 26/10/2007 pp 299–304
[9] Berten S, Hentschel S, Kieselbach K and Dupont P 2011 Experimental and Numerical Analysis of Pressure Pulsations and Mechanical Deformations in a Centrifugal Pump Impeller *Proceedings of the ASME-JSME-KSME 2011 Joint Fluids Engineering Conference* AJK-Fluids2011 vol 1 (Hamamatsu, Shizuoka, Japan: JSME) pp 297–306
[10] Duparchy F, Favrel A, Lowys P-Y, Landry C, Müller A, Yamamoto K and Avellan F 2015 Analysis of the part load helical vortex rope of a Francis turbine using on-board sensors *J. Phys. Conf. Ser.* **656** 012061
[11] Gao Z, Zhu W, Meng L, Zhang J, Zhang F, Pan L and Lu L 2017 Experimental Study of the Francis Turbine Pressure Fluctuations and the Pressure Fluctuations Superposition Phenomenon Inside the Runner *J. Fluids Eng.* **140** 041208-041208–9
[12] Kobro E 2010 *Measurement of pressure pulsations in Francis turbines* Ph. D. (Norwegian University of Science and Technology, Trondheim)
[13] Trivedi C, Agnalt E and Dahlhaug O G 2018 Experimental study of a Francis turbine under variable-speed and discharge conditions *Renew. Energy* **119** 447–58
[14] Bergan C, Goyal R, Cervantes M J and Dahlhaug O G 2016 Experimental Investigation of a High Head Model Francis Turbine During Steady-State Operation at Off-Design Conditions *IOP Conf. Ser. Earth Environ. Sci.* **49** 062018
[15] IEC 1999 *NEK IEC 60193 Hydraulic turbines, storage pumps and pump-turbines Model acceptance tests*
[16] Physikalisch-Technische Bundesanstalt (PTB) and German Calibration Service (DKD) 2014 Guideline DKD-R 6-1 Calibration of Pressure Gauges
[17] ISO/IEC GUIDE 98-3:2008(E) Guide to the expression of uncertainty in measurement (GUM:1995)
[18] Hessling J P 2006 A novel method of estimating dynamic measurement errors *Meas. Sci. Technol.* **17** 2740
[19] Elster C, Link A and Bruns T 2007 Analysis of dynamic measurements and determination of time-dependent measurement uncertainty using a second-order model *Meas. Sci. Technol.* **18** 3682
[20] Dunn P F 2014 *Measurement and Data Analysis for Engineering and Science, Third Edition* (CRC Press)